J. Fluid Mech. (2004), *vol.* 501, *pp.* 125–133. © 2004 Cambridge University Press
DOI: 10.1017/S0022112003007377 Printed in the United Kingdom

The effect of cylinder rotation and blockage ratio on the onset of periodic flows

By K. A. CLIFFE[1] AND S. J. TAVENER[2]

[1]Serco Assurance, Harwell International Business Centre, Didcot, Oxfordshire OX11 0RA, UK
[2]Department of Mathematics, Colorado State University, Fort Collins, CO 80623, USA

(Received 4 September 2003 and in revised form 8 November 2003)

The steady two-dimensional laminar flow past a stationary cylinder is well known to lose stability to a periodic flow at a supercritical Hopf bifurcation point as the flow rate is increased. It is less well known that the critical flow rate at which the instability occurs can be increased by rotating the cylinder about is own axis, and that at a fixed flow rate the vortex street can be eliminated entirely by sufficiently large rotation. We confine the flow between two parallel walls and report the effect of cylinder rotation on the Reynolds number and frequency at the Hopf bifurcation point. Two new, and somewhat surprising, results are that for stationary cylinders at large blockage ratios, the steady symmetric flow can restabilize above a critical Reynolds number, and that steady asymmetric flows exist.

1. Introduction

At sufficiently low flow rates, the two-dimensional flow of an incompressible Newtonian fluid past a cylinder is steady, laminar and symmetric about a plane through the centre of the cylinder and parallel to the far-field flow. This steady flow loses stability at a critical Reynolds number beyond which a periodic flow develops through a supercritical Hopf bifurcation point. This Hopf bifurcation point was located numerically by Jackson (1987) for flow in a laterally unbounded domain and by Chen, Pritchard & Tavener (1995) when the flow is confined between the parallel walls of a two-dimensional channel. A huge literature exists for flow past a cylinder as may be seen, for example, from the review of Williamson (1996) and the references cited therein.

Considerably less work has been performed on the flow past a rotating cylinder, and all work known to the authors has concentrated on approximating the flow in a laterally unbounded domain where there are no effects due to blockage ratio. Experimental work by Jaminet & Atta (1969) and numerical simulations by Badr, Dennis & Young (1989), Chew, Cheng & Luo (1995), Hu *et al.* (1996), Kang, Choi & Lee (1999), Barnes (2000), Chou (2000), Stojkocíc, Breuer & Durst (2002) and Mittel & Kumar (2003) have all shown that sufficiently large rotation of the cylinder can eliminate the vortex street downstream of the cylinder. In order to avoid the difficulties associated with the imposition of lateral boundary conditions approximating an unbounded domain, and to pose a problem that is perhaps even more amenable to well-controlled laboratory experiments, we confine the flow between two parallel walls. Large blockage ratios and rotation of the cylinder both conspire to make the wake very far from parallel and hence these flows are not amenable to analysis using the techniques for nearly parallel wakes pioneered by Monkewitz

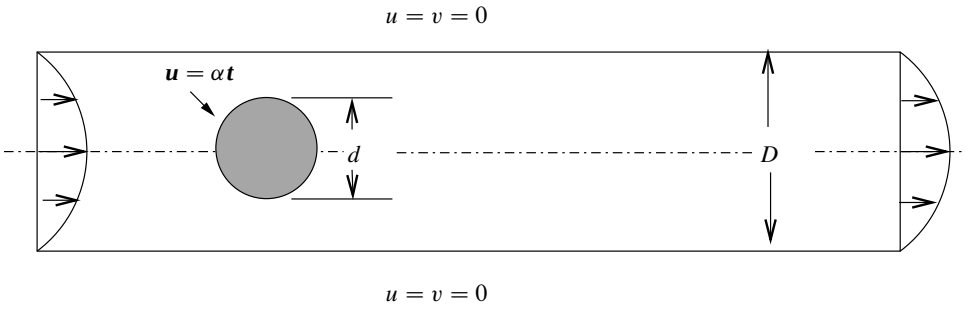

FIGURE 1. The flow domain.

and coworkers (see e.g. Monkewitz 1998; Monkewitz, Huerre & Chomaz 1993). The effects of finite blockage ratios are intriguing and introduce new phenomena, yet our results also strongly suggest that the observed behaviour in laterally unbounded domains can be understood in terms of the effect of cylinder rotation on the location of the Hopf bifurcation point.

2. Problem description

The flow domain is sketched in figure 1. For flow past a cylinder in a two-dimensional channel we define the blockage ratio B to be the ratio of the cylinder diameter to the channel width, i.e.

$$B = \frac{d}{D}. \tag{2.1}$$

The two-dimensional Navier–Stokes equations can be written in non-dimensional form as

$$R(\boldsymbol{u}_t + (\boldsymbol{u}\cdot\nabla)\boldsymbol{u}) = -\nabla p + \nabla^2\boldsymbol{u}, \tag{2.2}$$

$$\nabla\cdot\boldsymbol{u} = 0, \tag{2.3}$$

where $\boldsymbol{u}$ and p are the velocity and pressure fields respectively and

$$R = \frac{d\,U_d}{\nu}. \tag{2.4}$$

In order to facilitate comparison with flows in laterally unbounded domains (in the limit as $B \to 0$), the velocity scale was chosen to be the parabolic inlet velocity $u_{\text{inlet}}(y)$ averaged across the width of the cylinder, i.e.

$$U_d = \frac{1}{d}\int_{-d/2}^{d/2} u_{\text{inlet}}(y)\,\mathrm{d}y.$$

The rotation rate of the cylinder was non-dimensionalized in terms of the tangential velocity at the surface of the cylinder, u_{tang}, and we define

$$\alpha = \frac{u_{\text{tang}}}{U_d}. \tag{2.5}$$

Equations (2.2) and (2.3) were solved in weak form using the finite-element method. Isoparametric quadrilateral elements with biquadratic velocity interpolation and discontinuous linear pressure interpolation were used in all calculations. A fully developed parabolic flow was imposed at the inlet boundary and natural boundary

conditions (see e.g., p. 60, Gunzburger 1989) were applied at the outlet. No-slip boundary conditions were imposed along the channel walls and on the surface of the cylinder, i.e. $\boldsymbol{u} = \alpha \boldsymbol{t}$ at the surface of the cylinder, where $\boldsymbol{t}$ is the unit tangent vector to the cylinder surface.

3. Flow past a rotating cylinder in a channel

The effect of cylinder rotation on the location of the Hopf bifurcation point, and thereby on the onset of periodic solutions, is shown in figure 2(*a–c*) for a blockage ratio $B = 0.7$. In order to obtain an initial estimate of the location of one of these Hopf bifurcation points, steady solutions of equations (2.2), (2.3) were computed using the finite-element technique at fixed blockage ratio ($B = 0.7$) and rotation rate ($\alpha = 0$) for a range of Reynolds numbers. For each of these steady solutions, the 'most dangerous' eigenvalues of the linearized stability problem were computed using the Cayley transform techniques described by Cliffe, Garratt & Spence (1993). Hopf bifurcation was known to occur between two consecutive steady solutions when a pair of complex-conjugate eigenvalues crossed from the stable into the unstable half plane, or vice versa. For blockage ratio $B = 0.7$, a single pair of complex-conjugate eigenvalues was observed to cross from the stable to the unstable half-plane between $R = 90$ and 95, all other eigenvalues remaining stable. This single pair of complex-conjugate eigenvalues was observed to cross back into the stable half-plane between $R = 170$ and 180, all other eigenvalues remaining stable. (As will be discussed later, when a similar exercise was performed at blockage ratio $B = 0.6$ and $\alpha = 0$, a complex-conjugate pair of eigenvalues crossed into the unstable half-plane between $R = 100$ and 120. When the Reynolds number was further increased, a real eigenvalue crossed into the unstable half-plane between $R = 240$ and 260 and remained there when the unstable complex-conjugate pair crossed back into the stable half-plane between $R = 300$ and 320.) Given an initial guess of the marginally stable solution and the corresponding eigenvector, Hopf bifurcation points were computed using the extended system of Griewank & Reddien (1983) which has a regular solution at a Hopf bifurcation point. The entire path of Hopf bifurcation points was computed by coupling this extended system with the pseudo-arclength continuation technique of Keller (1977). The Strouhal number of the periodic flow is defined to be

$$S = \frac{df}{U_d}, \tag{3.1}$$

where f is the frequency of the periodic flow.

The critical Reynolds number at the Hopf bifurcation point is plotted against the non-dimensionalized rotation rate α in figure 2(*a*). The sign of the rotation is not significant, so we plot the critical Reynolds numbers at Hopf bifurcation points for $\alpha > 0$ only. Plotting the locus of Hopf bifurcation points for both positive and negative values of α produces a closed loop. Flows outside the closed loop of Hopf bifurcation points are stable with respect to time-dependent disturbances. The Strouhal number at the Hopf bifurcation point is plotted against $\alpha(>0)$ in figure 2(*b*), and the relationship between the critical Reynolds number and Strouhal number is plotted in figure 2(*c*).

Slow rotation of the cylinder about its own axis is seen to move the Hopf bifurcation point to slightly larger Reynolds number and slightly larger frequency. Thus, rotation stabilizes the steady flow, although for $\alpha \neq 0$ the flow is, of course, no longer symmetric. This effect is small until $|\alpha|$ approaches 1, at which point the critical Reynolds number

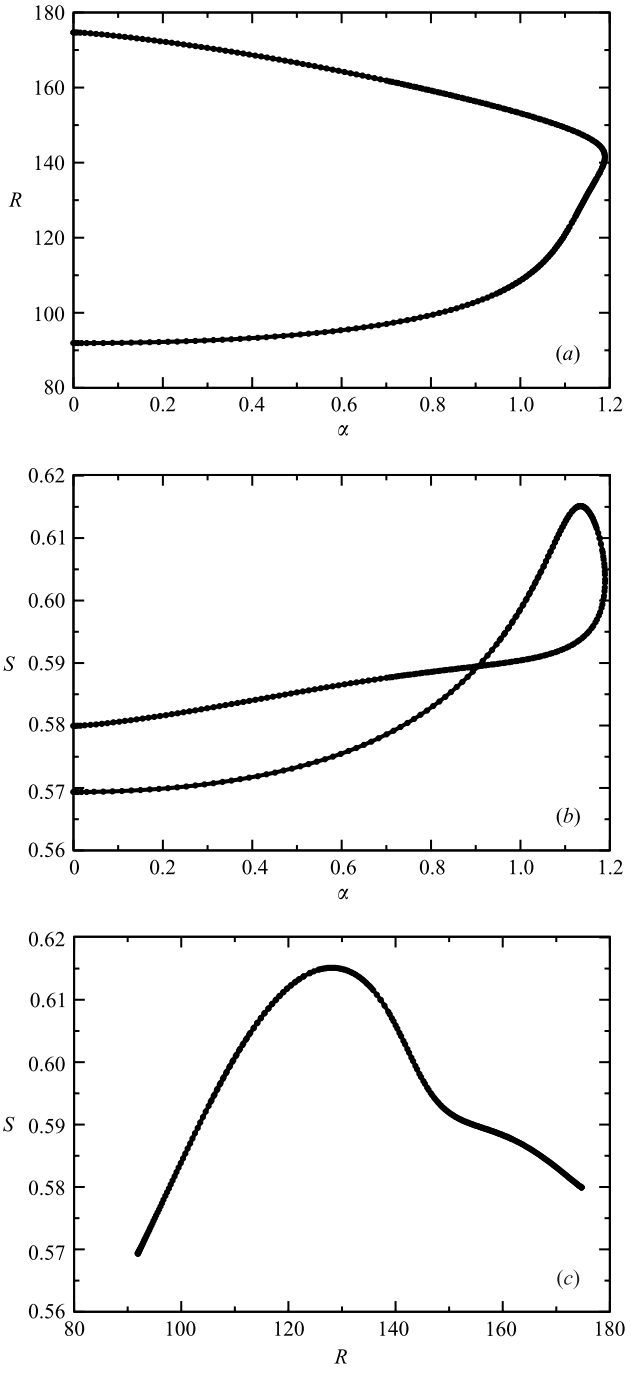

FIGURE 2. Hopf bifurcation points for blockage ratio, $B = 0.7$. (*a*) Reynolds number as a function of α; (*b*) Strouhal number as a function of α; (*c*) Strouhal number as a function of Reynolds number.

increases rapidly and the Strouhal number peaks. At $|\alpha| \sim 1.2$ there is a turning point in the path of Hopf bifurcation points and the upper Hopf bifurcation (at least initially) is such that periodic orbits exist only for Reynolds numbers between the two

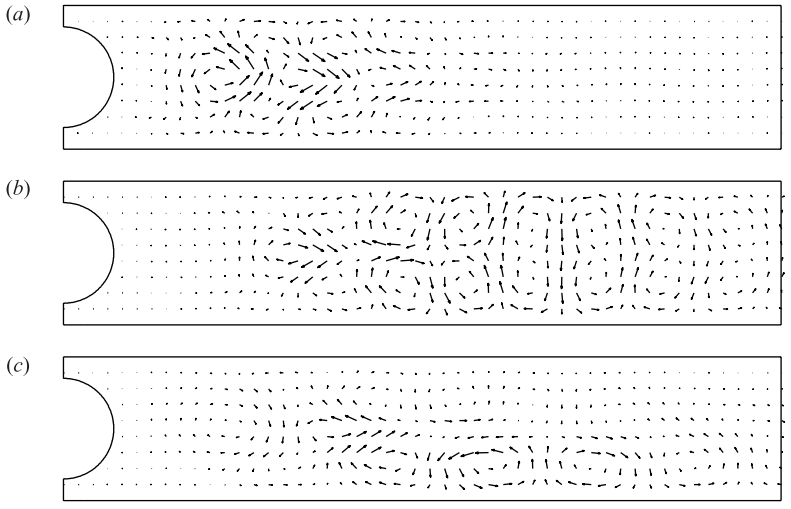

FIGURE 3. Velocity components of the null-eigenvector at the supercritical Hopf bifurcation point for $B = 0.7$. (*a*) $\alpha = 0$, $R = 92.0$; (*b*) $\alpha = 0$, $R = 174.7$; (*c*) $\alpha = 1.189$, $R = 140.7$.

Hopf bifurcation points. This has a number of ramifications. If $|\alpha| > 1.2$ the steady flow remains stable for all $R < 180.0$. For $92.0 < R < 175.0$, the periodic solution can be eliminated and a steady flow re-established by sufficiently large rotation of the cylinder. For fixed $|\alpha| < 1.2$, including $\alpha = 0$, the steady flow can be restabilized by *increasing* the Reynolds number sufficiently.

The real velocity components of the null eigenvector at the Hopf bifurcation points are shown in figures 3(*a*)–3(*c*) for $B = 0.7$ and $(\alpha, R) = (0, 92.0), (0, 174.7)$ and $(1.189, 140.7)$ respectively. When $\alpha = 0$ the streamwise velocity component of the real null-eigenvector is antisymmetric about the midplane and the cross-stream velocity component is symmetric. Significant components of the null eigenvector extend further downstream at the higher flow rate. When $\alpha \neq 0$, all components of the solution and eigenvector are asymmetric.

The corresponding streamlines and vorticity contours of the critical flows are shown in figures 4(*a–c*) and 5(*a–c*) respectively.

A convergence study was performed at $B = 0.7$, $\alpha = 0$ for both Hopf bifurcation points. The results are shown in table 1 and indicate that the errors in both the critical Reynolds numbers are less than 1% on the mesh with 3600 elements. The results for the Strouhal number are even more accurate. All computations reported here were performed using 3600 elements unless stated otherwise.

Time-dependent simulations were performed using an implementation of the variable-order, variable-time-step method of Byrne & Hindmarsh (1975) based on backward difference formulae of orders 1–5. The order and the time-step are chosen to ensure that the solution error is within a prescribed relative error tolerance, which was set to 0.001 for the computations reported here. A coarse mesh of 900 elements was used for expediency and thus the apparent critical values reported below do not coincide with the values shown in figure 2(*a*), but do agree with the locus of Hopf bifurcation points computed using the same 900 element mesh.

At a Reynolds number of 105, the flow was observed to be periodic for $0 < \alpha < 0.25$ and steady for $0.30 < \alpha < 0.38$; thus an increase in rotation rate suppressed the vortex

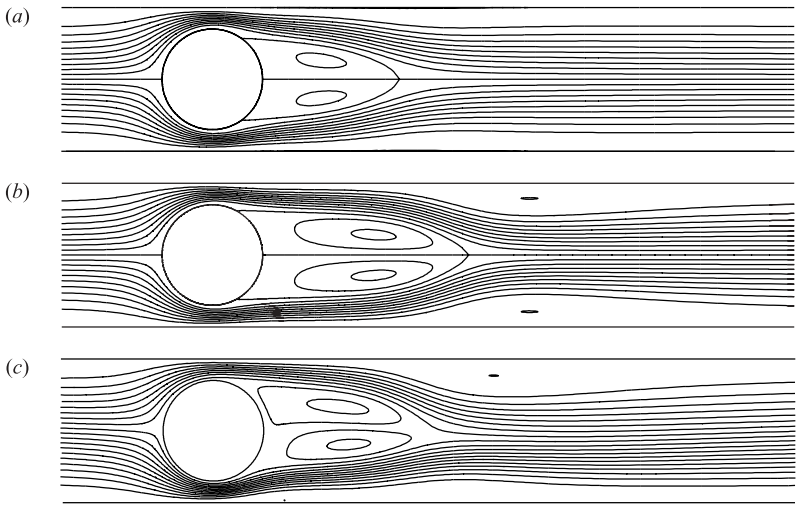

FIGURE 4. Streamlines at Hopf points at blockage ratio, $B = 0.7$. (*a*) $\alpha = 0$, $R = 92.0$, (*b*) $\alpha = 0$, $R = 174.7$; (*c*) $\alpha = 1.189$, $R = 140.7$. The contours are equally spaced.

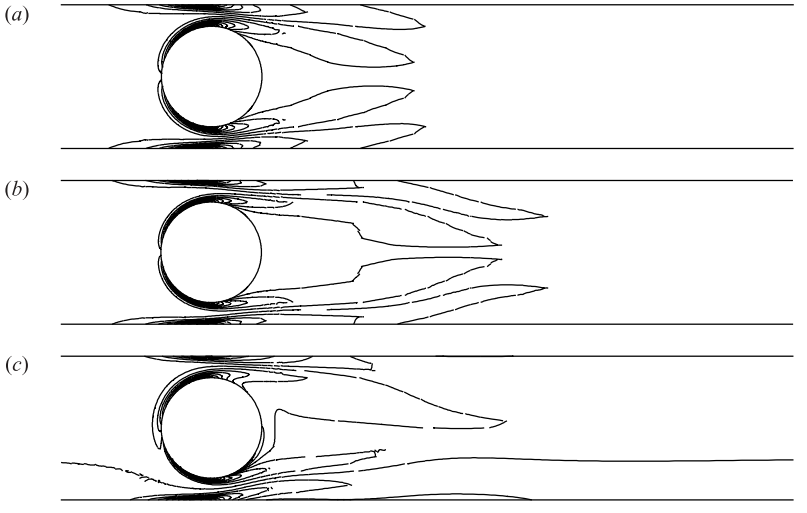

FIGURE 5. Contours of vorticity at Hopf points at blockage ratio, $B = 0.7$. (*a*) $\alpha = 0$, $R = 92.0$, (*b*) $\alpha = 0$, $R = 174.7$; (*c*) $\alpha = 1.189$, $R = 140.7$. The contours are equally spaced.

Number of elements	R	S
900	93.6882	0.5676
3600	91.9125	0.5694
8100	91.9811	0.5694
14400	91.9944	0.5694
900	154.1212	0.5724
3600	174.7059	0.5799
8100	174.7365	0.5806
14400	174.7156	0.5806

TABLE 1. Convergence study: the critical Reynolds number and Strouhal number are shown for a range of meshes.

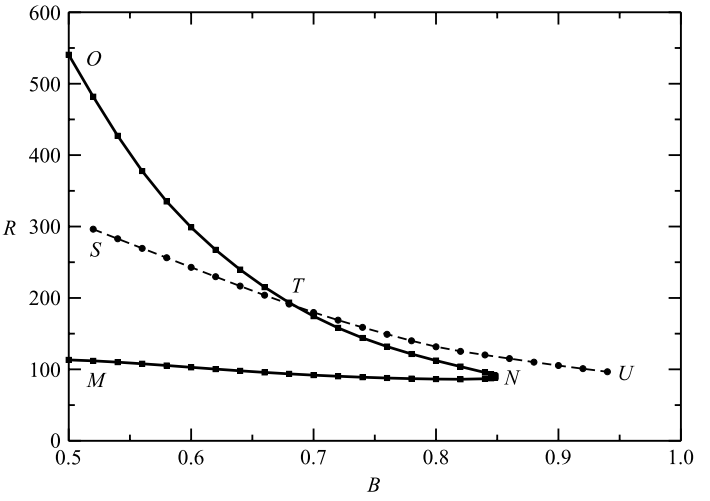

FIGURE 6. Loci of singular points as a function blockage ratio for a non-rotating cylinder, i.e. $\alpha = 0$. The solid line $MNTO$ is a path of Hopf bifurcation points. The dashed line STU is a path of symmetry-breaking bifurcation points on the steady symmetric branch. Their intersection, T, is a codimension-two point.

street. For $\alpha = 0$, the flow was observed to be periodic for $100 < R < 140$ and steady for $R = 160$; thus an increase in Reynolds number eliminated the vortex street.

The locus of Hopf bifurcation points for the flow past a non-rotating cylinder ($\alpha = 0$) as the blockage ratio B is varied is shown in figure 6. In this figure, $MNTO$ is the locus of Hopf bifurcation points and STU is a locus of symmetry-breaking bifurcation points at which a single real eigenvalue of the linearized stability problem crosses into the unstable plane. This symmetry-breaking bifurcation is disconnected for $\alpha \neq 0$ since the reflectional symmetry about the midplane is lost for non-zero rotation. The resulting path of limit points of the disconnected branch of solutions has not been computed.

The Hopf bifurcation points at larger Reynolds number are connected to the previously known Hopf bifurcation points computed by Chen *et al.* (1995), via a turning point in the path of Hopf bifurcation points at a blockage ratio, $B \sim 0.85$, which is labelled N in figure 6. Note that figure 2(a) represents a slice through figure 6 perpendicular to the blockage ratio axis at $B = 0.7$.

The nature of the Hopf bifurcations, either sub- or supercritical, was determined in two ways. (For definitions of sub- and supercritical Hopf bifurcations, see e.g., Golubitsky & Schaeffer 1985, p. 361.) The first was direct numerical simulation at Reynolds numbers immediately above and immediately below the critical value. The well-known difficulty of this approach is that the convergence rate near the Hopf bifurcation point is very slow. Secondly, a new method that combined finite-element discretization in space with spectral discretization in time was developed which allowed paths of periodic orbits to be computed as a parameter was varied. For example, at fixed blockage ratio and rotation rate, paths of periodic orbits could be calculated as the Reynolds number was varied. Further, periodic orbits arbitrarily close to the Hopf bifurcation point could be computed efficiently. By these means we were able to establish that (at least for $B > 0.7$) the periodic orbit which develops at the lower, supercritical Hopf bifurcation point decays at the upper Hopf bifurcation point. The latter technique is unable to determine the extent of the basin of attraction

FIGURE 7. Streamlines of the steady asymmetric flow at $B = 0.9, \alpha = 0, R = 114.3$. Contours of the streamfunction are equally spaced.

of the periodic orbit and, indeed, is equally capable of computing stable and unstable periodic orbits. Determining the basins of attraction of solutions to systems of partial differential equations such as those discussed here is not really practical and has not been attempted.

For blockage ratios less than 0.6, the steady symmetric flow loses stability at a critical Reynolds number (which depends on the blockage ratio) and remains unstable with respect to time-dependent disturbances for Reynolds numbers less than 300. For blockage ratios between 0.6 and 0.85, the symmetric flow restabilizes with respect to time-dependent disturbances at a Reynolds number less than 300. For blockage ratios greater than 0.85, the symmetric steady flow appears at first to remain stable. However, to conclude that the vortex street is damped by sufficiently large blockage ratio is to ignore the possibility of steady symmetry-breaking bifurcation. Steady symmetry-breaking bifurcation indeed occurs and is represented by the dashed line in figure 6. For blockage ratios exceeding 0.85, the first instability is no longer time-dependent, but is, rather, a steady symmetry-breaking instability. At a blockage ratio $B = 0.9$ for example, the steady symmetric flow loses stability to a steady asymmetric flow at the locus of symmetry-breaking bifurcation points. The streamlines for this flow at $R = 114.3$ are shown in figure 7. The linear stability of steady asymmetric flows was determined using the same technique of Cliffe *et al.* (1993) as was used for the steady symmetric flows. The steady asymmetric flow at $B = 0.9$ was found to be stable over a small interval in Reynolds number only, losing stability at $R = 114.5$ at a Hopf bifurcation point where a complex-conjugate pair of eigenvalues crosses into the unstable half of the complex plane. The steady O(2)-symmetric flow past a sphere in a pipe has been shown by Tavener (1994) and Cliffe, Spence & Tavener (2000) to lose stability with increasing flow rate at a steady symmetry-breaking bifurcation point. However, as far as the authors are aware, steady two-dimensional asymmetric flows past a cylinder were previously unknown.

Thus, the appealing conclusion that blockage ratio effects can eliminate the vortex street is incorrect. The complicated dynamics resulting from the interaction of the path of Hopf and symmetry-breaking bifurcation points and the codimension-two point T is as yet only partially explored. Simple stability arguments described in Golubitsky, Stewart & Schaeffer (1988, chap. XIX) suggest that for blockage ratios less than that at T there must be secondary bifurcation on the branches of periodic orbits and numerical techniques for locating these are being developed. The effect of rotation on this dynamical behaviour is again, as yet, unknown.

4. Conclusions

Rotation of a cylinder about its own axis has been shown to affect the critical Reynolds and Strouhal numbers at the Hopf bifurcation point in a manner that is consistent with existing experimental and numerical evidence. Restabilization of steady flows at large blockage ratios as the Reynolds number is increased was not expected, and has been shown to occur even for non-rotating cylinders. This feature should be observable experimentally. The appealing conclusion that sufficiently large

blockage ratio can eliminate the vortex street appears not to be true owing to Hopf bifurcation arising on previously unsuspected asymmetric branches. The mechanism producing the restabilization of steady flows has yet to be identified, as has the complex dynamical behaviour near the codimension-two point.

REFERENCES

Badr, H. M., Dennis, S. C. R. & Young, P. J. S. 1989 Steady and unsteady flow past a rotating circular cylinder at low Reynolds number. *Comput. Fluids* **17**, 579–609.

Barnes, F. H. 2000 Vortex shedding in the wake of a rotating circular cylinder at low Reynolds numbers. *J. Phys.* D **33**, L141–L144.

Byrne, G. D. & Hindmarsh, A. C. 1975 A polyalgorithm for the numerical solution of ordinary differential equations. *ACM Trans. Math. Soft.* **1**, 71–96.

Chen, J.-H., Pritchard, W. G. & Tavener, S. J. 1995 Bifurcation for flow past a cylinder between parallel plates. *J. Fluid Mech.* **284**, 23–41.

Chew, Y. T., Cheng, M. & Luo, S. C. 1995 A numerical study of flow past a rotating circular cylinder using a hybrid vortex scheme. *J. Fluid Mech.* **299**, 35–71.

Chou, M.-H. 2000 Numerical study of vortex shedding from a rotating cylinder immersed in a uniform flow field. *Intl J. Numer. Meth. Fluids* **32**, 545–567.

Cliffe, K. A., Garratt, T. J. & Spence, A. 1993 Eigenvalues of the discretized Navier-Stokes equations with application to the detection of Hopf bifurcations. *Adv. Comp. Maths* **1**, 337–356.

Cliffe, K. A., Spence, A. & Tavener, S. J. 2000 O(2)-symmetry breaking bifurcations: with application to flow past a sphere in a pipe. *Intl J. Numer. Meth. Fluids* **32**, 175–200.

Golubitsky, M. & Schaeffer, D. G. 1985 *Singularities and Groups in Bifurcation Theory*, vol. 1. Springer.

Golubitsky, M., Stewart, I. & Schaeffer, D. G. 1988 *Singularities and Groups in Bifurcation Theory*, vol. 2. Springer.

Griewank, A. & Reddien, G. 1983 The calculation of Hopf points by a direct method. *IMA J. Numer. Anal.* **3**, 295–304.

Gunzburger, M. D. 1989 *Finite Element Methods for Viscous Incompressible Flows*. Academic.

Hu, G.-H., Sun, D.-J., Yin, X.-Y. & Tong, B.-G. 1996 Hopf bifurcation in wakes behind a rotating and translating circular cylinder. *Phys. Fluids* **8**, 1972–1974.

Jackson, C. P. 1987 A finite-element study of the onset of vortex shedding in flow past variously shaped bodies. *J. Fluid Mech.* **182**, 23–45.

Jaminet, J. F. & Atta, C. W. V. 1969 Experiments on vortex shedding from rotating circular cylinders. *AIAA J.* **7**, 1817–1819.

Kang, S., Choi, H. & Lee, S. 1999 Laminar flow past a rotating circular cylinder. *Phys. Fluids* **11**, 3312–3321.

Keller, H. B. 1977 Numerical solution of bifurcation and nonlinear eigenvalue problems. In *Applications of Bifurcations Theory* (ed. P. Rabinowitz), pp. 359–384. Academic.

Mittel, S. & Kumar, B. 2003 Flow past a rotating cylinder. *J. Fluid Mech.* **476**, 303–334.

Monkewitz, P., Huerre, P. & Chomaz, J.-M. 1993 Global linear stability analysis of weakly non-parallel shear flows. *J. Fluid Mech.* **251**, 1–20.

Monkewitz, P. A. 1998 The absolute and convective nature of instability in two-dimensional wakes at low Reynolds numbers. *Phys. Fluids* A **5**, 999–1006.

Stojkocíc, D., Breuer, M. & Durst, F. 2002 Effect of high rotation rates on the laminar flow around a circular cylinder. *Phys. Fluids* **14**, 3160–3178.

Tavener, S. J. 1994 Stability of the O(2)-symmetric flow past a sphere in a pipe. *Phys. Fluids* A **6**, 3884–3892.

Williamson, C. H. K. 1996 Vortex dynamics in the cylinder wake. *Annu. Rev. Fluid Mech.* **28**, 477–539.